World Journal of Gastroenterology

Online Submissions: http://www.wjgnet.com/esps/
wjg@wjgnet.com
doi:10.3748/wjg.v19.i20.3027

World J Gastroenterol 2013 May 28; 19(20): 3027-3042
ISSN 1007-9327 (print) ISSN 2219-2840 (online)

ORIGINAL ARTICLE

Matrix metalloproteinase-9 in the initial injury after hepatectomy in mice

Norifumi Ohashi, Tomohide Hori, Florence Chen, Sura Jermanus, Akimasa Nakao, Shinji Uemoto, Justin H Nguyen

Norifumi Ohashi, Akimasa Nakao, Gastroenterological Surgery, Nagoya University Graduate School of Medicine, Nagoya, Aichi 466-8550, Japan
Tomohide Hori, Shinji Uemoto, Divisions of Hepato-Pancreato-Biliary, Transplant and Pediatric Surgery, Department of Surgery, Kyoto University Graduate School of Medicine, Kyoto 606-8507, Japan
Florence Chen, Sura Jermanus, Department of Neuroscience, Mayo Clinic, Jacksonville, FL 32224, United States
Justin H Nguyen, Division of Transplant Surgery, Department of Transplantation, Mayo Clinic in Florida, Jacksonville, FL 32224, United States
Author contributions: Nguyen JH designed this study; Ohashi N performed the surgery and the assays, wrote the initial draft, and performed statistical analysis; Hori T performed the additional surgeries for the second assays to confirm the initial results; Chen F and Jermanus S helped with the assays; Nguyen JH and Hori T contributed to further drafts; Nakao A, and Uemto S provided important advice for the research; Nguyen JH supervised the research.
Supported by Partially by Grants to Nguyen JH from the Deason Foundation (Sandra and Eugene Davenport, Mayo Clinic CD CRT-II), the AHA (0655589B) and NIH (R01NS051646-01A2); and the Grant to Hori T from the Uehara Memorial Foundation (200940051)
Correspondence to: Tomohide Hori, MD, PhD, Divisions of Hepato-Pancreato-Biliary, Transplant and Pediatric Surgery, Department of Surgery, Kyoto University Graduate School of Medicine, 54 Shogoinkawara-cho, Sakyo-ku, Kyoto 606-8507, Japan. horit@kuhp.kyoto-u.ac.jp
Telephone: +81-75-7513651 Fax: +81-75-7513106
Received: December 17, 2012 Revised: January 7, 2013
Accepted: February 5, 2013
Published online: May 28, 2013

Abstract

AIM: To investigate the role of matrix metalloproteinase (MMP)-9 in the pathogenesis of postoperative liver failure (PLF) after extended hepatectomy (EH).

METHODS: An insufficient volume of the remnant liver (RL) results in higher morbidity and mortality, and a murine model with 80%-hepatectomy was used. All investigations were performed 6 h after EH. Mice were first divided into two groups based on the postoperative course (*i.e.*, the PLF caused or did not), and MMP-9 expression was measured by Western blotting. The source of MMP-9 was then determined by immunohistological stainings. Tissue inhibitor of metalloproteinase (TIMP)-1 is the endogenous inhibitor of MMP-9, and MMP-9 behavior was assessed by the experiments in wild-type, MMP-9(-/-) and TIMP-1(-/-) mice by Western blotting and gelatin zymography. The behavior of neutrophils was also assessed by immunohistological stainings. An anti-MMP-9 monoclonal antibody and a broad-spectrum MMP inhibitor were used to examine the role of MMP-9.

RESULTS: Symptomatic mice showed more severe PLF (histopathological assessments: 2.97 ± 0.92 *vs* 0.11 ± 0.08, $P < 0.05$) and a higher expression of MMP-9 (71085 ± 18274 *vs* 192856 ± 22263, $P < 0.01$). Non-native leukocytes appeared to be the main source of MMP-9, because MMP-9 expression corresponding with CD11b positive-cell was observed in the findings of immunohistological stainings. In the histopathological findings, the PLF was improved in MMP-9(-/-) mice (1.65% ± 0.23% *vs* 0.65% ± 0.19%, $P < 0.01$) and it was worse in TIMP-1(-/-) mice (1.65% ± 0.23% *vs* 1.78% ± 0.31%, $P < 0.01$). Moreover, neutrophil migration was disturbed in MMP-9(-/-) mice in the immunohistological stainings. Two methods of MMP-9 inhibition revealed reduced PLF, and neutrophil migration was strongly disturbed in MMP-9-blocked mice in the histopathological assessments (9.6 ± 1.9 *vs* 4.2 ± 1.2, $P < 0.05$, and 9.9 ± 1.5 *vs* 5.7 ± 1.1, $P < 0.05$).

CONCLUSION: MMP-9 is important for the process of PLF. The initial injury is associated with MMP-9 derived from neutrophils, and MMP-9 blockade reduces PLF. MMP-9 may be a potential target to prevent PLF after

EH and to overcome an insufficient RL.

Key words: Matrix metalloproteinase; Shear stress; Sinusoidal injury; Hepatectomy; Portal hypertension

Ohashi N, Hori T, Chen F, Jermanus S, Nakao A, Uemoto S, Nguyen JH. Matrix metalloproteinase-9 in the initial injury after hepatectomy in mice. *World J Gastroenterol* 2013; 19(20): 3027-3042 Available from: URL: http://www.wjgnet.com/1007-9327/full/v19/i20/3027.htm DOI: http://dx.doi.org/10.3748/wjg.v19.i20.3027

INTRODUCTION

Liver resection is considered the standard treatment for primary malignant tumors and liver metastases. Currently, advanced surgical techniques for hepatectomy, development of preoperative evaluation and improvements in intensive postoperative care have resulted in a decline in perioperative morbidity and mortality. However, postoperative liver failure (PLF) still occurs despite these developments. Extended hepatectomy (EH) has the advantage of high curability, but increases morbidity and mortality compared with more limited resections[1]. The volume of the remnant liver (RL) is correlated with perioperative morbidity and mortality[1]. PLF is also related to the patient's condition[2]. The rationale for PLF is the overall recovery course after EH. Prognosis of PLF in insufficient RL after EH is poor[1,2].

The mechanism of progressive PLF after EH is not fully understood. The main pathway of failure of liver regeneration is still controversial, and it is unclear how excessive apoptosis or progressive necrosis is attributable to insufficient RL after EH. Matrix metalloproteinases (MMPs) are a family of zinc-containing neutral proteases that are capable of degrading the extracellular matrix and basement membrane. Among MMPs, MMP-9, also known as gelatinase B, is well characterized[3-5]. Expression of MMP-9 is reported to be associated with several pathophysiological conditions, such as rheumatoid arthritis[6], atherosclerosis[6], encephalopathy[7] and tumor invasion[8,9]. Recent studies have demonstrated that MMP-9 plays a pivotal role in ischemia/reperfusion injury in the liver transplantation field[4,10]. We hypothesized that MMP-9 plays a role in the pathogenesis of PLF after EH accompanied by postoperative shear stress due to portal hypertension and insufficient RL, and we previously reported the results of our preliminary study[11]. In this study, we examined the initial pathway of necrosis in the PLF process and MMP-9 expression in the early phase after EH by using an experimental mice model. In addition, we evaluated the efficacy of MMP-9 blockade on initial injury in the liver by deleting MMP-9 in the mouse, using a monoclonal antibody and a broad spectrum MMP inhibitor.

MATERIALS AND METHODS

Animals

Male C57BL/6 mice [wild-type (WT), 10-14 wk old] purchased from Jackson Laboratory (Bar Harbor, ME), were housed in a conventional mouse room with a 12-h light/dark cycle, food, and water. MMP-9(-/-) mice, which were a gift from Dr. Roberts Senior (Washington University, St. Louis, MO), and tissue inhibitor of metalloproteinase (TIMP)-1(-/-) mice, which were purchased from Jackson Laboratory were used. Both knock-out strains had the background of C57/BL/6, and all mice were bred in our secure animal facility. All experimental protocols were approved by the ethical committee of the Mayo Clinic (Protocol No. IACUC 24907) in accordance with the National Institutes of Health Guide for the Care and Use of Laboratory Animals.

Eighty percent-partial hepatectomy in mice

Surgical procedures for the murine hepatectomy model are well established, and our method has been described in detail elsewhere[12]. For 80%-partial hepatectomy (PH), the left posterior, left and right anterior, and right posterior lobes were resected. In brief, under general anesthesia using isoflurane, liver lobes were mobilized after laparotomy. A hemostatic clip (Teleflex Medical, Triangle Park, NC) was applied across the pedicle at the base of the liver lobes instead of ligation, and liver lobes were cut distal to the applied clip. Only laparotomy was performed as the sham control group. Before abdominal closure, 2 mL of warm saline was administered intraperitoneally. Cephalexin (30 mg/kg) and buprenorphine (0.1 mg/kg) were given subcutaneously. To preserve the same quality throughout the series, all procedures for presented data were performed only by Ohashi N. To confirm the presented data, Hori T repeated this study including 90%-PH. Postoperatively, mice were housed under a controlled temperature, humidity, and light with free access to food and water.

First, we performed 90%-PH in 50 WT mice, and all mice died at the early postoperative period. In this study, we employed 80%-PH as the relevant clinical model. Ninety-percent-PH showed greater damage in the preliminary study, but we considered that 10%-RL was clinically irrelevant. Paradoxically, some survivors without any symptoms were observed after 80%-PH.

We then performed 80%-PH in 38 WT mice and sham surgery in 12 WT mice, to evaluate the postoperative course. In the following experiments, 80%-PH was performed with 20 age-matched WT mice, 19 MMP-9(-/-) mice and 20 TIMP-1(-/-) mice.

Focal and/or patchy necrosis is an important finding after PH[13-16], and progressive necrosis is found from the early postoperative period after EH[13,14,16]. In this study, all of the mice were sacrificed at 6 h after 80%-PH. The RL was harvested and divided for histological analysis (formalin and frozen fixation) and protein analysis (snap frozen at -80 ℃). Serum samples were collected and sep-

arated by using Microtainer tubes (BD, Franklin Lakes, NJ).

MMP-9 inhibition experiment using anti-MMP-9 monoclonal antibody and the broad-spectrum MMP inhibitor GM6001

The WT mice were treated with 3 mg/kg of anti-MMP-9 neutralizing monoclonal antibody (clone 6-6B, EMD, Gibbstown, NJ) by intravenous injection 1 h before 80%-PH (MMP-9 mAb group, n = 6). In the control mice, the same volume of non-immunized murine IgG of the same isotype (EMD, Gibbstown, NJ) was injected in the same manner (control IgG group, n = 6). In another experiment, a broad spectrum MMP-inhibitor, GM6001 (Millipore, Billerica, MA) (100 mg/kg), diluted in 10% dimethyl sulfoxide (DMSO) was administrated intraperitoneally 2 h before 80%-PH (GM6001 group, n = 10). Ten percent DMSO was injected in the control mice in the same manner as for GM6001 (vehicle group, n = 10).

Biochemical analysis

Serum levels of aspartate aminotransferase (AST) and alanine aminotran-saminase (ALT) were determined by a commercially available kinetic detection kit (Pointe Scientific, INC, Canton, MI), and total bilirubin (T-Bil) levels were determined by the QuantiChrom™ Bilirubin Assay Kit (BioAssay Systems, Heyward, CA).

Western blotting analysis

Liver samples were homogenized in a buffer containing 10 mmol/L Tris-HCl (pH 7.4), 150 mmol/L NaCl, 1% Triton-X, 0.1% sodium dodecyl sulfate (SDS), 1 mmol/L ethylene diamine tetra-acetic acid (EDTA), 1 mmol/L ethylene glycol tetra-acetic acid, 1 mmol/L phenylmethylsulfonyl fluoride, and protease and phosphatase inhibitors. Homogenates were centrifuged at 105000 *g* for 1 h at 4 ℃. Supernatants were collected and protein concentration was determined by BCA assay (Pierce, Rockford, IL). Forty micrograms of protein was separated *via* SDS-polyacrylamide gel electrophoresis (SDS-PAGE) and transferred to a polyvinylidene difluoride (PVDF) membrane (Millipore, Bedford, MA). Membranes were blocked with 5% nonfat milk in TBS-T [20 mmol/L Tris (pH 7.4), 500 mmol/L NaCl, and 0.05% Tween-20] and probed using an antibody for MMP-9 (R and D, Minneapolis, MN), and then they were incubated with peroxidase-conjugated secondary antibodies (Santa Cruz Biotechnology, Santa Cruz, CA) followed by enhanced chemi-luminescence (ECL) or ECL-plus reagent (Amersham Biosciences, Piscataway, NJ). Equal loading was confirmed by immunoblotting using glyceraldehyde-3-phosphate dehydrogenase (GAPDH) monoclonal antibody (IMGENEX, San Diego, CA) on the same membrane. Signals were quantified using the ImageQuant program (Molecular Dynamics, Sunnyvale, CA).

Gelatin zymography

The RL extracts were analyzed by gelatin zymography with affinity chromatography to characterize gelatinase activity. In brief, 400 μg of extract samples were incubated with 100 μL of Gelatin-Sepharose 4B (GE Healthcare) and equilibrated buffer containing 50 mmol/L Tris-HCL pH 7.5, 150 mmol/L NaCl, 5 mmol/L $CaCl_2$, 0.02% Tween-20, and 10 mmol/L EDTA for 2 h at 4 ℃. After multiple washing, gelatin-Sepharose beads were resuspended in the same volume of 2X zymography sample buffer (Bio-Rad Laboratories, Hercules, CA) and loaded on 10% SDS-PAGE gels containing 1 mg/mL of gelatin (Bio-Rad Laboratories) After electrophoresis, the gel was washed with 2.5% Triton X-100 for renaturing twice for 30 min, and it was then incubated in development buffer (Bio-Rad Laboratories) for 20 h at 37 ℃. After incubation, the gel was fixed and stained with 0.5% Coomassie Blue R-250 (Bio-Rad Laboratories) for 1 h and destained with 10% acetic acid in 40%-methanol solution. Gelatinase zymography standards (Millipore, Billerica, MA) were used for the positive control.

Histology and immunohistochemical staining

Formalin-fixed liver specimens were embedded in paraffin, and 5-μm sections were stained with hematoxylin and eosin (HE). Immunohistochemical (IHC) staining for CD11b (MAC-1) and CD68 was performed on frozen sections (5 μm), while paraffin sections were used for desmin, myeloperoxidase (MPO) and MMP-9 single staining. Antigen retrieval heating with citric acid (pH 6.0) was performed after deparaffinization with paraffin sections. For horseradish peroxidase based staining with 3,3' diaminobenzidine tetrahydrochloride (DAB) (DAKO, Carpinteria, CA), 0.3% H_2O_2 was added to quench endogenous peroxidase activity, and an ABC kit (Vector Laboratories Inc, Burlingame, CA) was used during the staining procedure according to the manufacturer's instructions. For dual staining, sections were blocked with 5% bovine serum albumin (BSA) in PBS. The antibodies for MMP-9 (AF909), intercellular adhesion molecule 1 (ICAM-1) (AF796), CD11b (clone M1/70) (R and D, Minneapolis, MN), CD68 (clone FA-11), desmin (Abcam, Cambridge, MA), and MPO (Ab-1) (Thermo scientific, Fremont, CA) were incubated for the primary reaction. Alexa Fluor 568 donkey anti-goat IgG (H + L), Alexa Fluor 488 donkey anti-rabbit IgG and Alexa Fluor 488 donkey anti-rat antibody (Invitrogen, Carlsbad, CA) were incubated for the secondary reaction. In each experiment, BSA solutions without antibodies were applied for a negative control.

Histological analysis

The HE sections were digitally scanned with the Scanscope XT system and analyzed with Aperio Imagescope software (Aperio Technologies, Inc., Vista, CA). Histological areas were blindly counted and measured with three randomly selected fields approximately 3 mm^2 in each section. The positivity of DAB staining for MMP-9 was automatically calculated using the positive pixel count function with Imagescope software with 10 ran-

domly selected fields with the reference to the presence of necrosis, respectively. The value was indicated by the percentage of positive pixels out of the total pixels. The number of infiltrated granulocytes was evaluated in five randomly-captured 40 high power fields in each section with an Olympus BX50 fluorescence microscope (Olympus Optical, Tokyo, Japan).

In situ zymography

In situ gelatinolytic activity was performed on cryostat sections (20-μm thickness) using the EnzChek Gelatinase assay kit (Molecular Probes, Eugene, Oregon, United States). Sections were incubated with 20 μg/mL fluorescent conjugated gelatin (DQ gelatin) in reaction buffer (50 mmol/L Tris-HCl, 150 mmol/L NaCl, 5 mmol/L $CaCl_2$, and 0.2 mmol/L sodium azide) for 2 h at 37 ℃. After being washed with PBS three times, they were fixed in 4% paraformaldehyde in PBS. We incubated sections with GM6001 (100 μmol/L) prior to DQ gelatin incubation as a negative control in each experiment. Sections were mounted with Vectashield (Vector Laboratories Inc, Burlingame, CA). Gelatinase activity was visualized using fluorescent microscopy (Olympus BX50, Japan).

Statistical analysis

Data are presented as the mean ± SE. Statistical comparisons were performed using ANOVA followed by the two-sample *t*-test with Bonferroni adjustment. A P value < 0.05 was considered statistically significant.

RESULTS

Necrosis is a pivotal event for PLF in the RL after 80%-PH

Murine behavior in hepatic failure has been well described[17,18]. Mice with intrahepatic-hemorrhage and necrosis were observed to be sick and inactive, whereas mice without such injury were asymptomatic and active. We classified these mice into groups based on these findings as follows below. Mice were divided into two groups; asymptomatic (Group Ⅰ) and symptomatic (Group Ⅱ).

We performed 80%-PH in 38 WT mice and sham surgery in 12 WT mice to compare the difference in the RL with or without PLF at several time points after 80%-PH. Among these mice, we randomly selected five asymptomatic mice which were active, nimble and reactive to stimulation, and six symptomatic mice which were sick and inactive, slow-moving and sluggish 6 h after 80%-PH. As shown in Figure 1A and B, multiple necrotic foci with microhemorrhage in the middle zone were observed in the symptomatic mice, while a small amount of necrosis was observed in the asymptomatic mice. These HE findings are consistent with a previous report[19]. We measured the area of necrosis as an objective marker of liver injury. The area of necrosis (2.97% ± 0.92% *vs* 0.11% ± 0.08%, $P < 0.05$) (Figure 1C) and the number of necrotic foci (3.60 ± 0.87/mm^2 *vs* 0.26 ± 0.17/mm^2, $P < 0.01$) in the RL were significantly larger in symptomatic mice than those in asymptomatic mice (Figure 1D). Serum levels of AST (785 ± 15 IU/L *vs* 452 ± 39 IU/L, $P < 0.01$) (Figure 1E), ALT (744 ± 135 IU/L *vs* 328 ± 77 IU/L, $P < 0.05$) (Figure 1F), and T-Bil (4.45 ± 0.63 mg/dL *vs* 1.41 ± 0.19 mg/dL, $P < 0.01$) (Figure 1G) were significantly higher in symptomatic mice than those in asymptomatic mice. These results clearly indicated that symptomatic mice were in the process of PLF as shown by the increase in AST and ALT levels and hyperbilirubinemia. In some mice, which failed to recover even 6 h after 80%-PH, multiple necroses might have been responsible for the process of PSL in this model. Enhanced necrosis was observed in the RL at the late phase (12 h or later, data not shown), and these preliminary data confirmed that the necrotic pathway is progressive. In addition, intrahepatic-hemorrhage was observed in most of the necrotic lesions, which suggested the possibility that the initial sinusoid endothelial cell injury leading to sinusoidal breakdown is attributable to necrosis in the RL. In our model, dehiscence of sinusoids and loss of continuity of endothelial cells were observed in ICAM-1 immunostaining, which was strongly positive in endothelial cells (Figure 1H).

We preformed retrospective analysis of perioperative factors including the resected liver weight/body weight and surgery time with 11 mice whose prognosis was predictable. Perioperative factors were not different between asymptomatic and symptomatic mice, but the resected liver weight/body weight ratio in the symptomatic mice tended to be larger than that in the asymptomatic mice (3.8% ± 0.1% *vs* 3.5% ± 0.1%, $P = 0.06$). It is possible that the extent of hepatectomy is an important factor for postoperative liver injury after EH.

Macro- and microscopically, we confirmed the preservation of vascularization in the RL, immediately after 80%-PH by sodium fluorescent perfusion via the portal vein and abdominal aorta, to exclude model specific effects including surgical issues. In addition, we observed similar histological findings after 80%-PH with the traditional suture ligation method[13] (data not shown). These results demonstrated that the process of PSL after EH was widely and histologically characterized by RL necrosis, and was probably initialized as early onset sinusoid breakdown following progressive necrosis of hepatocytes.

MMP-9 expression is enhanced in RL dysfunction 6 h after 80%-PH and is associated with liver necrosis

We compared MMP-9 expression in the RL between asymptomatic mice and symptomatic mice at 6 h. Enhanced MMP-9 expression was confirmed in symptomatic mice after EH compared with that in the asymptomatic mice after EH and sham surgery mice as shown by Western blotting analysis ($P < 0.01$) (Figure 2). IHC showed that MMP-9 expression was mainly observed in round-shaped cells in the liver parenchyma and necrotic areas, and was less common in stellate-shaped cells. A small amount of MMP-9 expression was observed in hepatocytes compared with the above-mentioned cells (Figure 3A and B). To evaluate the association of necrosis and MMP-9 in liver tissue, we compared the expression level of MMP-9 between 10 randomly selected fields (3 mm^2)

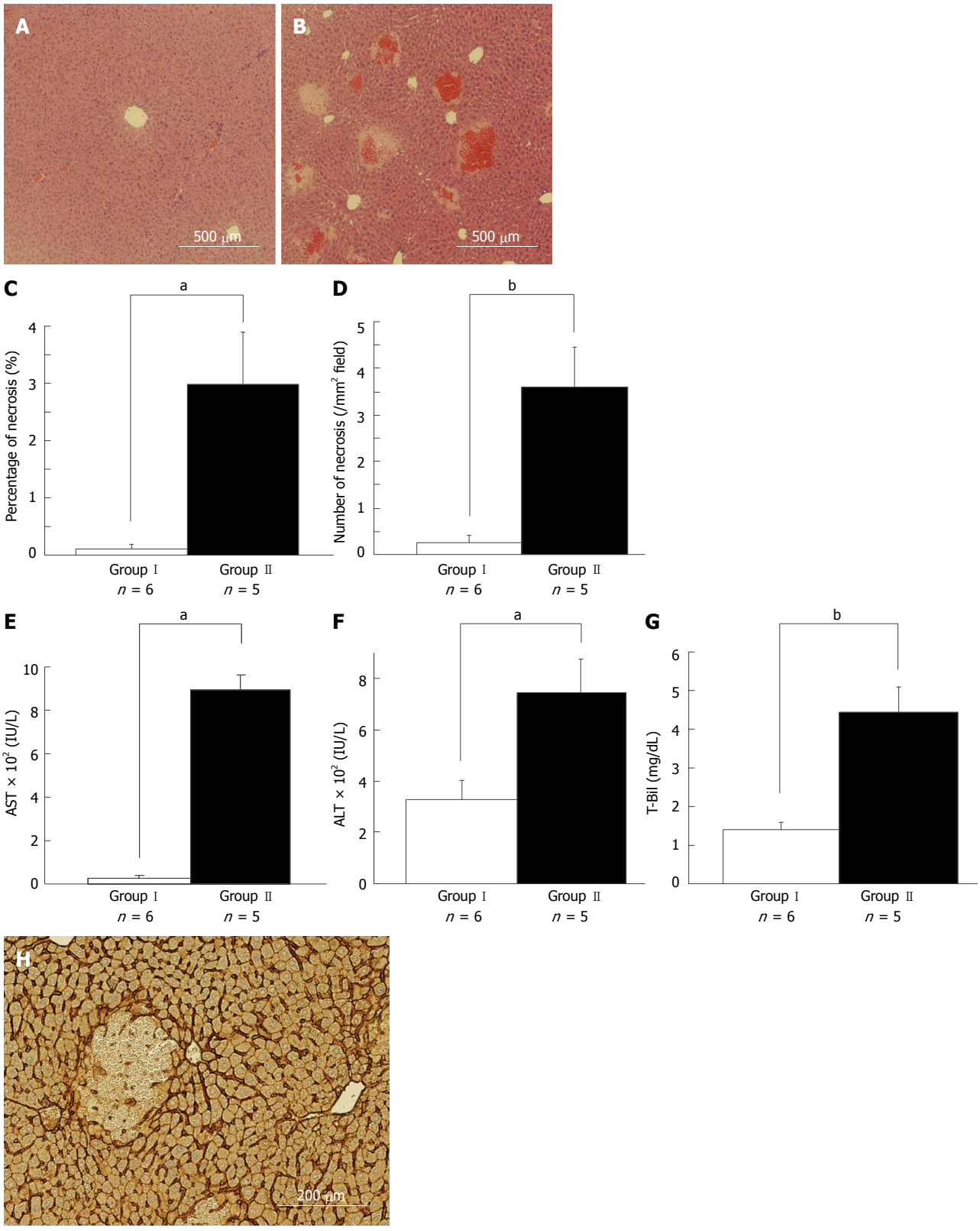

Figure 1 Necrosis is a pivotal event for postoperative liver failure in the remnant liver after 80%-partial hepatectomy. There were histological and hematological differences between asymptomatic and symptomatic mice suspected as having postoperative liver failure 6 h after 80%-partial hepatectomy (PH) (A, B). Representative images of the remnant liver (RL) 6 h after 80%-PH in asymptomatic mice (A) and symptomatic mice (B) are shown. Significant multiple necroses with microhemorrhage were observed in the middle zone in symptomatic mice (B), while no obvious liver damage was observed in asymptomatic mice (A). The percentage area of necrosis (C) and the number of necrosis in each mm^2 (D) in the RL were confirmed. Necrotic areas were significantly larger and more prevalent in symptomatic mice liver compared with asymptomatic mice. Serum levels of aspartate aminotransferase (AST) (E), alamine aminotransferase (ALT) (F) and total bilirubin (T-Bil) (G) 6 h after 80%-PH are shown. AST, ALT and T-Bil levels were significantly elevated in symptomatic mice compared with those in asymptomatic mice. Representative image of immunohistochemistry of intercellular adhesion molecule-1 (ICAM-1) in the RL 6 h after 80%-PH is shown (H). ICAM-1 expression was clearly observed, particularly in the sinusoid lining in areas without necrosis. We observed a breakdown in sinusoid structure with hemorrhage in necrotic areas after 80%-PH in mice, $^{a}P < 0.05$, $^{b}P < 0.01$ *vs* asymptomatic mice.

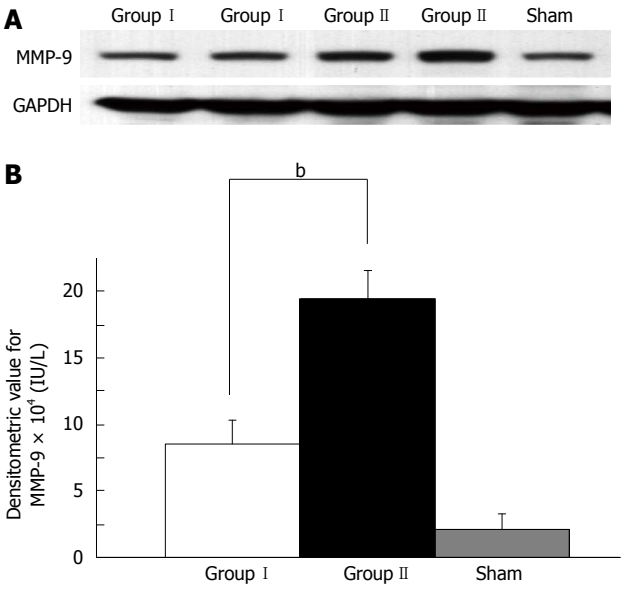

Figure 2 Western blotting analyses for matrix metalloproteinase-9 were performed in the remnant liver in asymptomatic mice and symptomatic mice after 80%-partial hepatectomy. Representative image (A) and histograms (B) of Western blotting analyses for matrix metalloproteinase-9 (MMP-9) are shown. MMP-9 protein expression in the liver was enhanced in symptomatic mice in the process of postoperative liver failure compared with that in asymptomatic mice after extended hepatectomy and sham-treated mice (^bP < 0.01 between Groups Ⅰ and Ⅱ).

of areas with necrosis and those without necrosis in IHC sections. Enhanced MMP-9 expression was observed in the areas including necrosis compared with those without necrosis ($P < 0.05$, Figure 3C). This result suggested that MMP-9 expression is associated with necrosis in the RL after EH.

Main source of MMP-9 is CD11b-positive nonnative leukocytes in the RL 6 h after 80%-PH

To determine the source of MMP-9, we performed dual immunofluorescent analysis with MMP-9 and various cell marker antibodies in the liver. CD68 and desmin were used as specific markers for Kupffer cells and hepatic stellate cells in immunostaining, respectively. MMP-9 expression was not observed in CD68-positive Kupffer cells, while MMP-9 expression was partially confirmed in desmin-positive hepatic stellate cells (Figure 4A-F). In addition, we clearly detected MMP-9 expression corresponding with CD11b positive-cells, which are generally expressed in nonnative leukocytes in the liver including monocytes, granulocytes and macrophages (Figure 4G-I). These results suggested that MMP-9 was expressed in the RL 6 h after 80%-PH, and it appeared to be mainly produced by leukocytes that had migrated from the outside of the liver, similar to that described in a liver ischemia/reperfusion injury model[20].

MMP-9 deletion ameliorates initial injury in the RL 6 h after 80%-PH

TIMP-1 is an endogenous inhibitor of MMP-9. We performed 80%-PH in 20 WT, 19 MMP-9(-/-) and 20

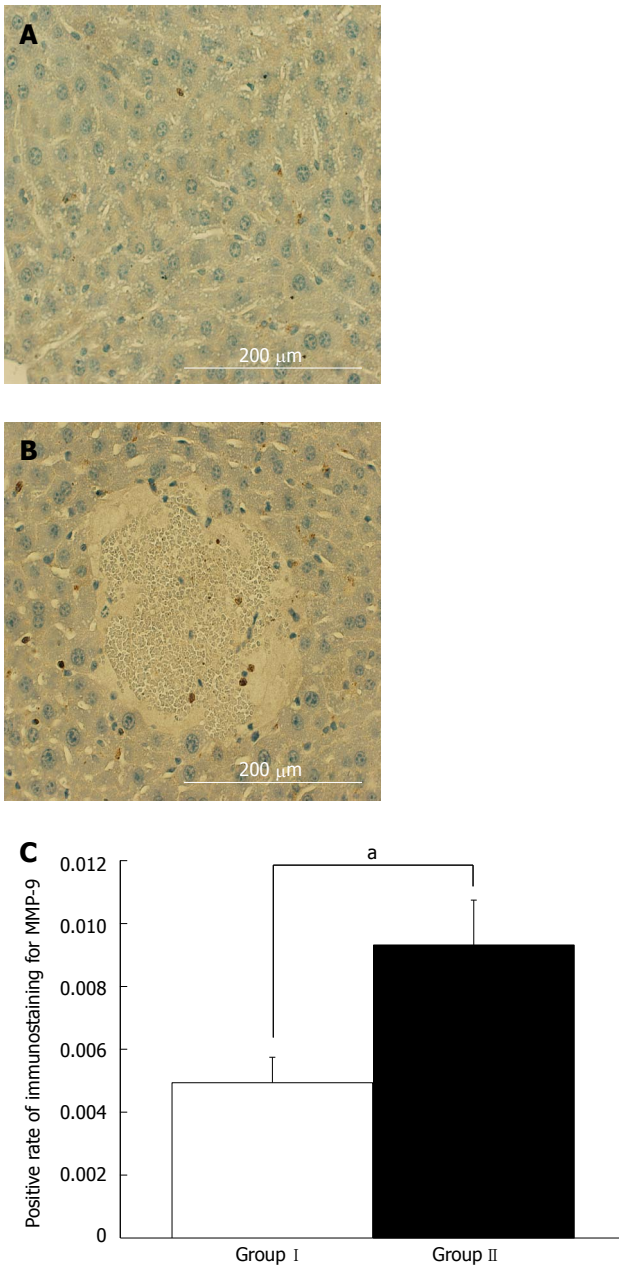

Figure 3 Immunohistochemical analysis for matrix metalloproteinase-9 in the remnant liver in symptomatic mice after 80%-partial hepatectomy was performed. A: Representative images of matrix metalloproteinase-9 (MMP-9) staining in an area without necrosis; B: A necrotic area in the same sample are shown. Histograms of the results of distribution analysis show MMP-9 expression; C: Enhanced expression was observed in the areas close to necrosis compared with areas without necrosis in damaged RL (^aP < 0.05 between Groups Ⅰ and Ⅱ).

TIMP-1(-/-) mice to compare the difference in the RL 6 h after 80%-PH. Among these mice, we randomly selected samples from 15 WT, 15 MMP-9(-/-) and 14 TIMP-1(-/-) mice. To evaluate the effects of MMP-9 on the initial injury in the RL, we compared the area (percentage) of necrosis and the number of necrotic foci in the RL among these samples. There were significantly fewer and smaller necrotic lesions in MMP-9(-/-) mice compared with WT mice and TIMP-1(-/-) mice (area, WT: 1.65% ± 0.23%; MMP-9(-/-): 0.65% ± 0.19%;

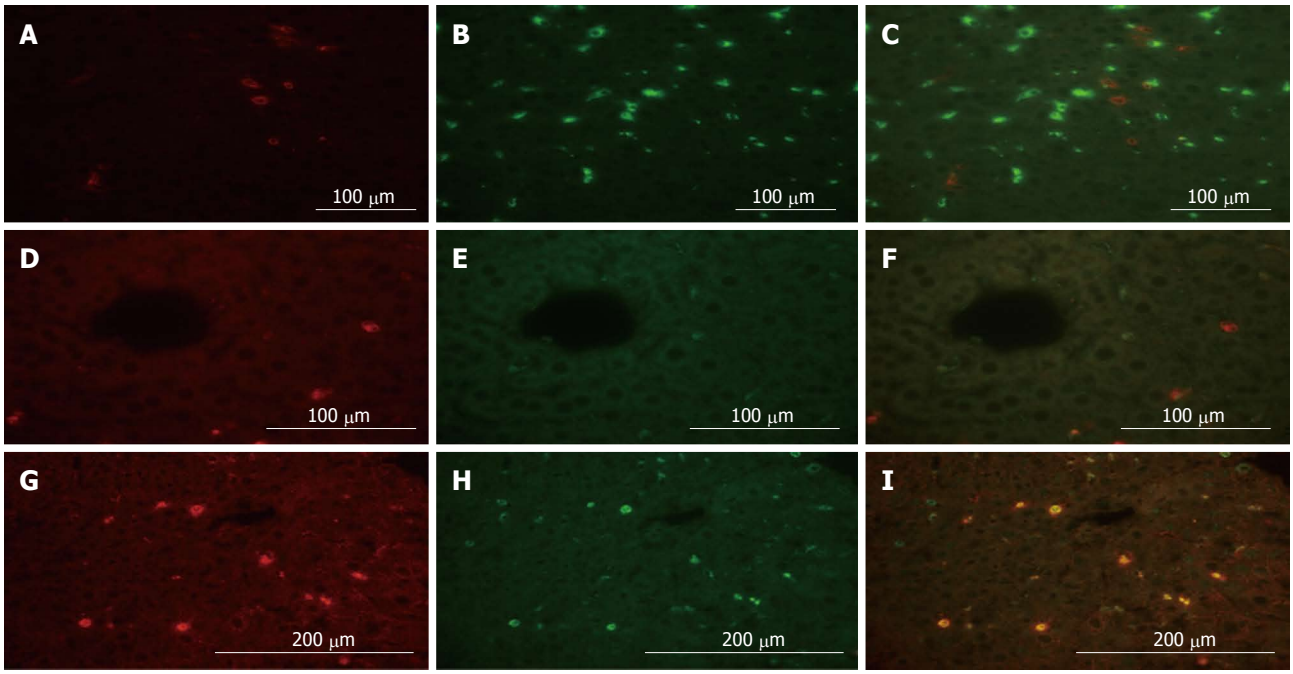

Figure 4 Localization analysis of matrix metalloproteinase-9 by dual immune-fluorescence in the remnant liver after 80%-partial hepatectomy is shown. A: Fluorescent microscopy images of matrix metalloproteinase-9 (MMP-9) labeled in red (Alexa Fluor 568); B: CD68 labeled in green (Alexa Fluor 488); C: A merged image of MMP-9 and CD68 staining are shown; D: MMP-9 labeled in red (Alexa Fluor 568); E: Desmin labeled in green (Alexa Fluor 488); and F: A merged image of MMP-9 and desmin are shown; G: MMP-9 labeled in red (Alexa Fluor 568); H: CD11b labeled in green (Alexa Fluor 488); I: A merged image of MMP-9 and CD11b are shown. Protein expression of MMP-9 was mainly localized in CD11b-positive cells and desmin-positive cells to some degree.

TIMP-1(-/-): 1.78% ± 0.31%; MMP-9(-/-) *vs* WT: $P < 0.01$; MMP-9(-/-) *vs* TIMP-1(-/-): $P < 0.01$), (number of necrotic foci, WT: 1.34 ± 0.20/mm^2; MMP-9(-/-): 0.68 ± 0.16/mm^2; TIMP-1(-/-): 1.50 ± 0.30/mm^2; MMP-9(-/-) *vs* WT: $P < 0.05$; MMP-9(-/-) *vs* TIMP-1(-/-): $P < 0.05$) (Figure 5). There was no significant difference in necrosis between WT and TIMP-1(-/-) mice. The levels of AST (WT: 520 ± 69 IU/L; MMP-9(-/-): 482 ± 76 IU/L; TIMP-1(-/-): 636 ± 58 IU/L) and ALT (WT: 544 ± 73 IU/L; MMP-9(-/-): 466 ± 92 IU/L; TIMP-1(-/-): 566 ± 54 IU/L) were lowest in MMP-9(-/-) mice, but this was not statistically significant among the groups. Additionally, T-Bil levels showed a similar tendency (WT: 2.72 ± 0.36 mg/dL; MMP-9(-/-): 2.23 ± 0.27 mg/dL; TIMP-1(-/-): 2.76 ± 0.28 mg/dL). In Western blotting and gelatin zymography analysis, MMP-9 deletion of protein expression and activity in MMP-9(-/-) mice were confirmed. Protein expression of MMP-9 in WT mice was similar to that in TIMP-1(-/-) mice (Figure 6A). In gelatin zymography analysis, a distinct pro-form of MMP-9 and a slightly active form of MMP-9 were detected in WT and TIMP-1(-/-) mice (Figure 6B). No difference in MMP-9 activity was detected in the genotypes. Since there was no change in MMP bands among the groups because of the principle of protein separation by SDS-PAGE in zymography, we performed *in situ* gelatin zymography to examine the gelatinolytic activity *in situ*. We observed reduced gelatinolytic activity in MMP-9(-/-) mice and enhanced activity in TIMP-1(-/-) mice compared with that in WT mice (Figure 6C-E). MMP-9 deletion, which suppresses gelatinolytic activity, was associated with the amelioration of formation of necrosis and necrotic progression in the RL after 80%-PH. However, TIMP-1 deletion, which induces the enhancement of gelatinolytic activity, did not exacerbate initial injury of the RL after EH. These results suggested that the involvement of TIMP-1 in inhibition of MMP activity appeared to be limited to PLF 6 h after EH. We investigated survival after 80%-PH was performed in WT, MMP-9(-/-) and TIMP-1(-/-) mice, but a significant survival benefit was not observed by MMP-9 deletion ($P \geqslant 0.05$).

MMP-9 deletion inhibits the accumulation of neutrophils in the RL 6 h after 80%-PH

To evaluate the effect of MMP-9 deletion on cell kinetics, we investigated whether neutrophil migration after 80%-PH has an effect on the RL in WT, MMP-9(-/-) and TIMP-1(-/-) mice. We performed immunofluorescence staining for myeloperoxidase (MPO) to investigate this issue. As shown in Figure 7A, MPO-positive neutrophils could be easily recognized by characteristic staining patterns in cytoplasmic azurophilic granules, and MPO was also positive in liver tissue macrophages (Kupffer cells)[21]. Because of the difficulty in distinguishing between infiltrated neutrophils in the liver parenchyma and those that were adhered to the sinusoidal wall, accumulated neutrophils were counted in liver tissue. We observed significantly fewer neutrophils in MMP-9(-/-) mice (3.3 ± 0.4) than in WT (7.6 ± 1.3) and TIMP-1(-/-) mice (6.1 ± 1.0; each value per 40 high-power field; WT *vs* MMP-9(-/-), $P < 0.01$; MMP-9(-/-) *vs* TIMP-1(-/-), $P < 0.05$) (Figure 7B-E). There were no differences in ICAM-1 expression

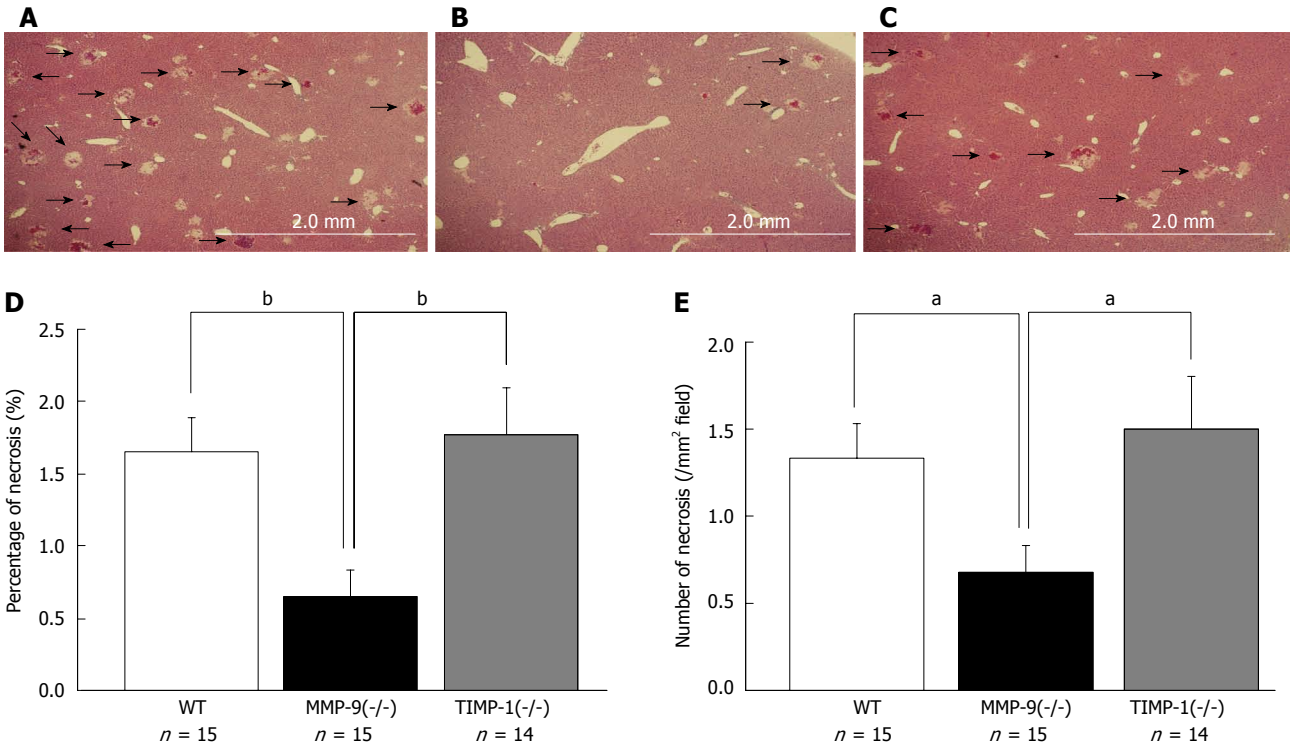

Figure 5 Histological analysis between wild-type, matrix metalloproteinase-9(-/-), and tissue inhibitor of metalloproteinase-1(-/-) mice 6 h after 80%-partial hepatectomy were performed. Representative images of the remnant liver (RL) 6 h after 80%-PH in wild-type (WT) (A), matrix metalloproteinase-9 (MMP-9)(-/-) (B), and tissue inhibitor of metalloproteinase-1 (TIMP-1)(-/-) mice (C) are shown. Samples that included necrosis were selected for this figure. The percentage (D) and the number of necrotic foci per mm^2 (E) of the necrotic area in the RL are shown. We observed significantly smaller and less necrotic foci in MMP-9(-/-) mice compared with WT and TIMP-1(-/-) mice ($^aP < 0.05$, $^bP < 0.01$ *vs* WT and TIMP-1).

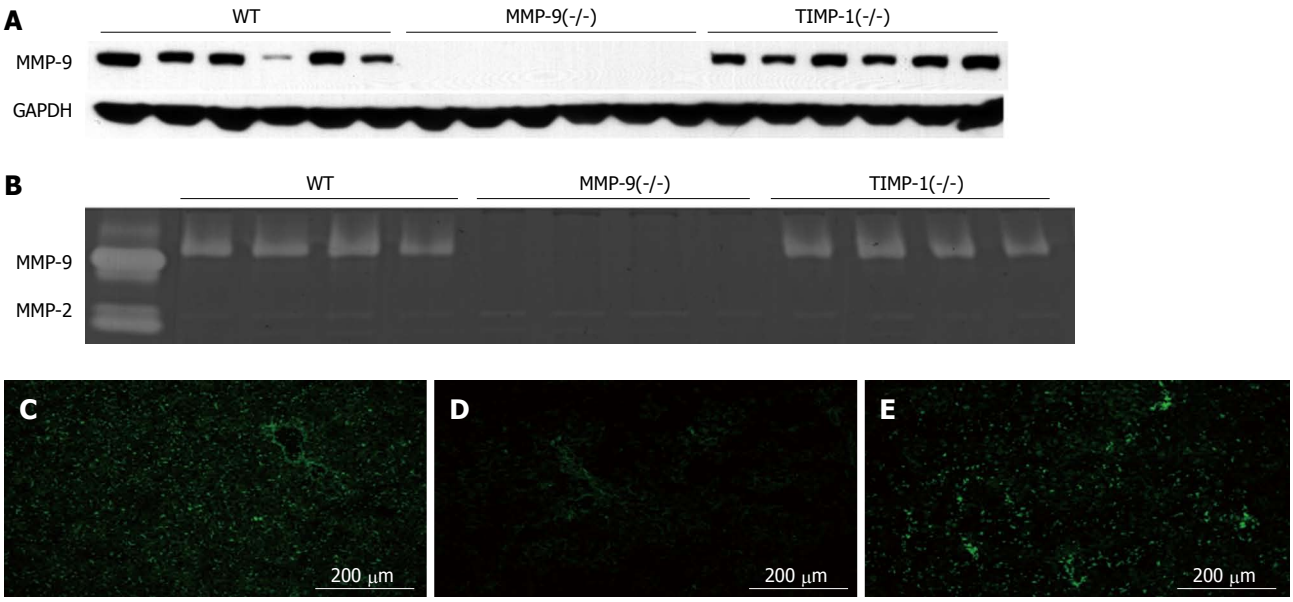

Figure 6 Matrix metalloproteinase-9 activity in the remnant liver with wild-type, matrix metalloproteinase-9(-/-), and tissue inhibitor of metalloproteinase-1(-/-) mice 6 h after 80%-partial hepatectomy is shown. A: Western blotting analysis for matrix metalloproteinase-9 (MMP-9) and glyceraldehyde 3-phosphate dehydrogenase (GAPDH) for a loading control was performed. The expression of MMP-9 in wild-type (WT) and tissue inhibitor of metalloproteinase-1 (TIMP-1)(-/-) mice and deletion in MMP-9(-/-) mice were observed at the protein level; B: Gelatin zymography analysis is shown; C-E: Pro-form MMP-9 activity and a slightly active form of MMP-9 were detected in WT and TIMP-1(-/-) mice. The activity of MMP-2 was the same depending on its genotype. *In situ* gelatin zymography analysis using DQ gelatin for gelatinolytic activity in the liver tissue is shown. A reduction in gelatinolytic activity in MMP-9(-/-) mice and enhancement in TIMP-1(-/-) mice are observed.

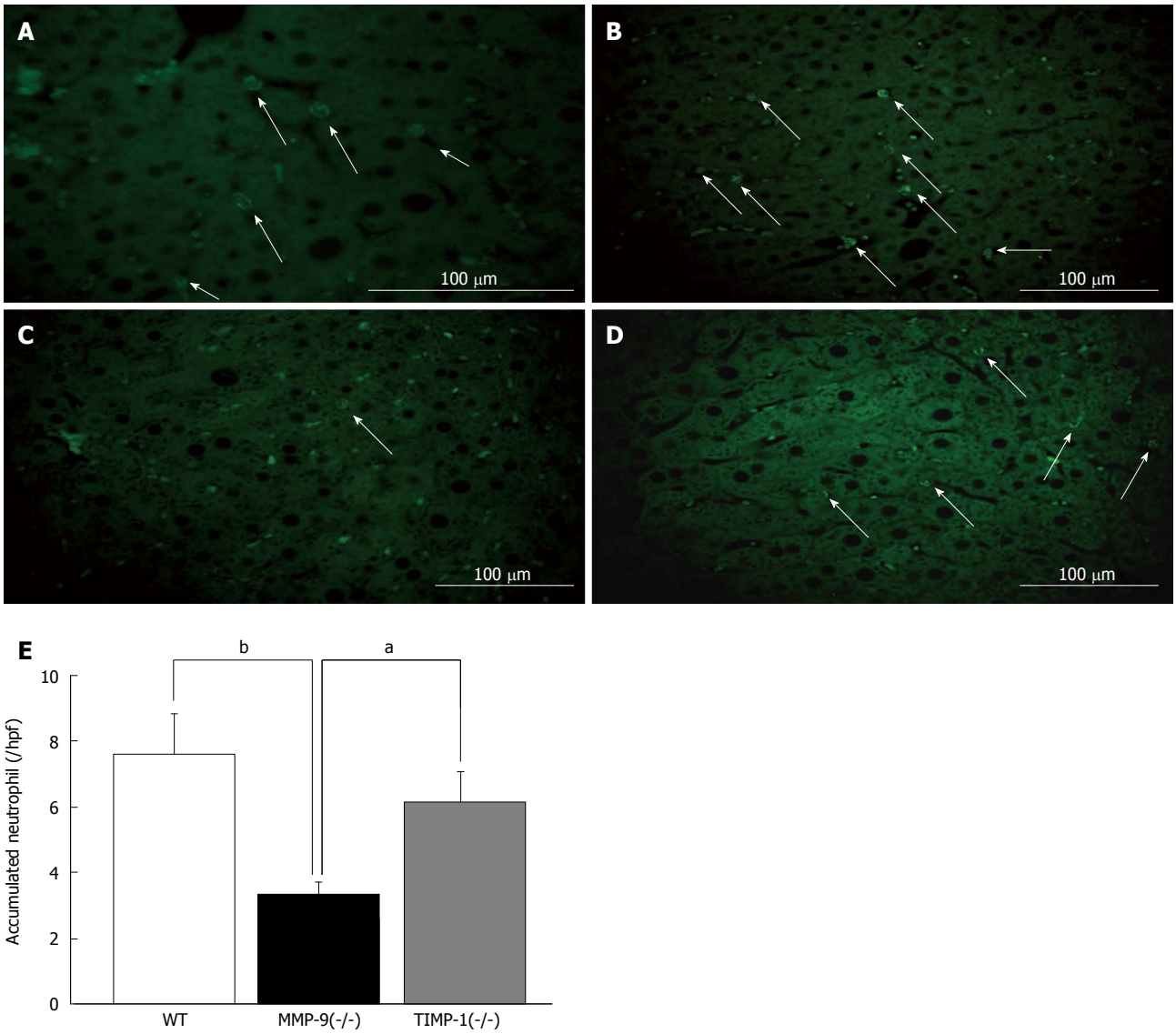

Figure 7 Immunohistochemistry analysis for accumulated neutrophils with myeloperoxidase staining between wild-type, matrix metalloproteinase-9(-/-) and tissue inhibitor of metalloprote-inase-1(-/-) mice 6 h after 80%-partial hepatectomy was performed. Myeloperoxidase (MPO) staining labeled in green (Alexa Fluor 488) is shown (A). Cytoplasmic azurophilic granules were characteristically stained in neutrophils. Representative images of MPO staining on a remnant liver (RL) section in green in wild-type (WT) (B), matrix metalloproteinase-9 (MMP-9)(-/-) (C), tissue inhibitor of metalloproteinase-1 (TIMP-1)(-/-) mice (D) are shown. A histogram of the number of accumulated neutrophils in the liver is shown. We observed significantly fewer neutrophils in the RL in MMP-9(-/-) mice than in WT and TIMP-1(-/-) mice ($^{a}P < 0.05$, $^{b}P < 0.01$ *vs* WT and TIMP-1) (E).

among WT, MMP-9(-/-) and TIMP-1(-/-) mice in Western blotting and IHC analysis (data not shown). These results suggested that MMP-9 deletion was associated with a decrease in migrated neutrophils in the liver, which was related to an amelioration of the initial injury in the RL after EH, and probably an infiltrating process seemed to be influenced. Therefore, MMP-9 might play a supportive role for infiltration of neutrophils into the RL at the early phase after EH.

Inhibition of MMP-9 by a monoclonal antibody of MMP-9 and the broad-spectrum MMP inhibitor GM6001 ameliorate initial injury of the liver 6 h after 80%-PH

Investigation of inhibition of MMP-9 *in vivo* was performed by two different methods using a blocking monoclonal antibody and a broad-spectrum MMP inhibitor (GM6001). Each treatment clearly improved survival curves after 80%-PH ($P < 0.01$). In the RL, there were significantly smaller and fewer necrotic lesions in the monoclonal antibody-injected mice (mAb group) than in the control IgG-injected mice (control IgG group) (area: 0.17% ± 0.15% *vs* 1.81% ± 0.66%, $P < 0.05$, Figure 8A; number of foci: 0.23 ± 0.16/mm^2 *vs* 1.23 ± 0.44/mm^2, $P < 0.05$, Figure 8B). Serum levels of AST, ALT and T-Bil were lower in the monoclonal antibody-injected mice than those in the control IgG-injected mice, but this not statistically significant ($P \geqslant 0.05$). We confirmed suppression of gelatinolytic activity in the mAb group by *in situ* gelatin zymography compared with that in the control IgG group (Figure 8C and D). There were significantly

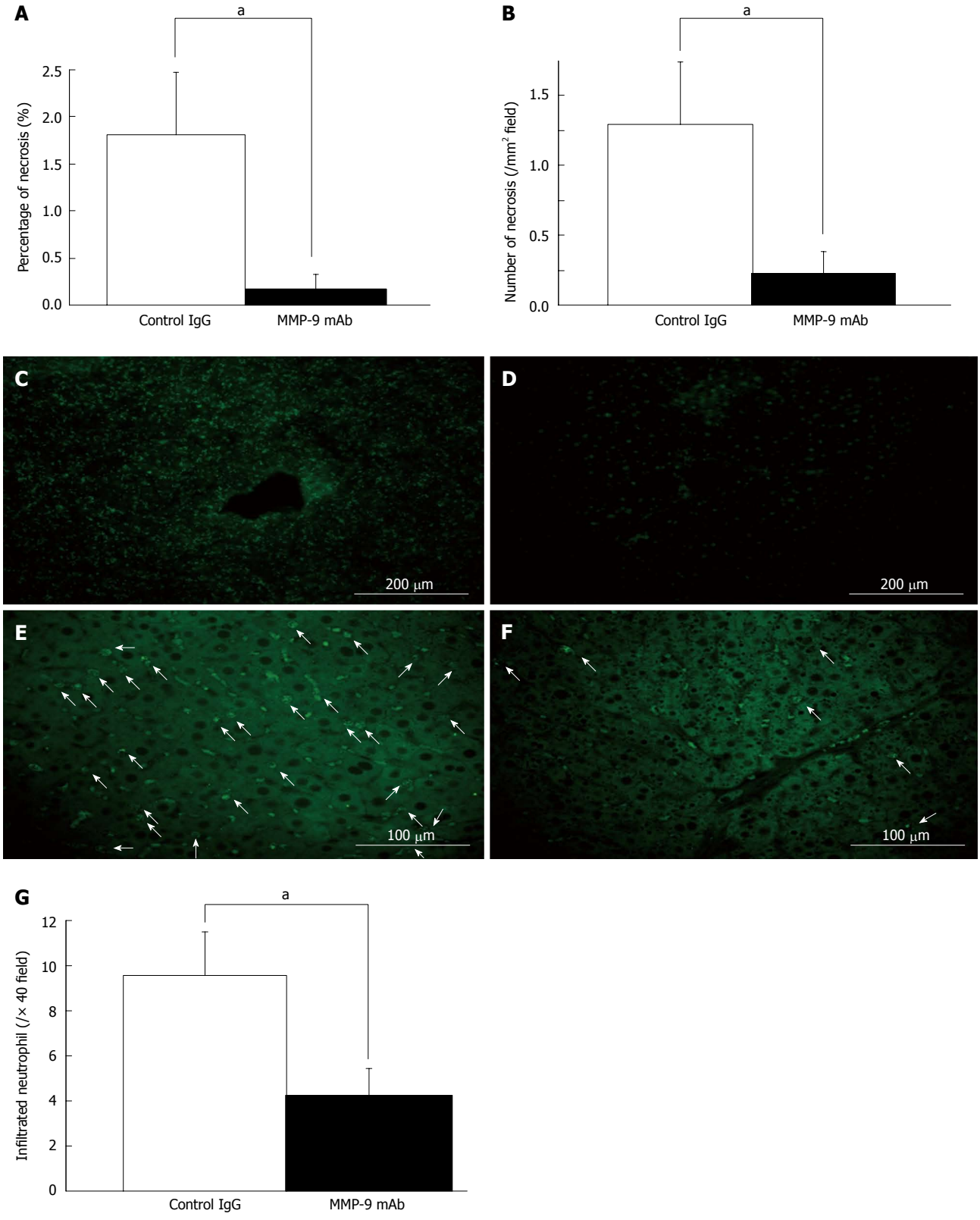

Figure 8 Inhibition of matrix metalloproteinase-9 by a monoclonal antibody of matrix metalloproteinase-9. We investigated the outcome of inhibition of matrix metalloproteinase-9 (MMP-9) by monoclonal antibody (mAb) in 80%-partial hepatectomy (PH) in mice, and performed histological analysis of liver necrosis 6 h after 80%-PH (A, B). Liver damage was significantly reduced in the group with mAb compared with that in the control IgG group. Serum levels of aspartate aminotransferase, alamine aminotransferase and total bilirubin were lower in the mAb-treated mice, but this was not significant. Representative images of *in situ* gelatin zymography analysis with DQ gelatin revealed that gelatinolytic activity was suppressed in the mAb-treated mice (D) compared with that in control IgG-treated mice (C). Representative images of myeloperoxidase staining on remnant liver (RL) sections in control IgG-treated mice (E) and mAb-treated mice (F) are shown. A histogram of the number of accumulated neutrophils in the RL 6 h after 80%-PH shows that there are significantly fewer neutrophils in mAb-treated mice than in IgG-treated controls (G) ($^aP < 0.05$ *vs* IgG group).

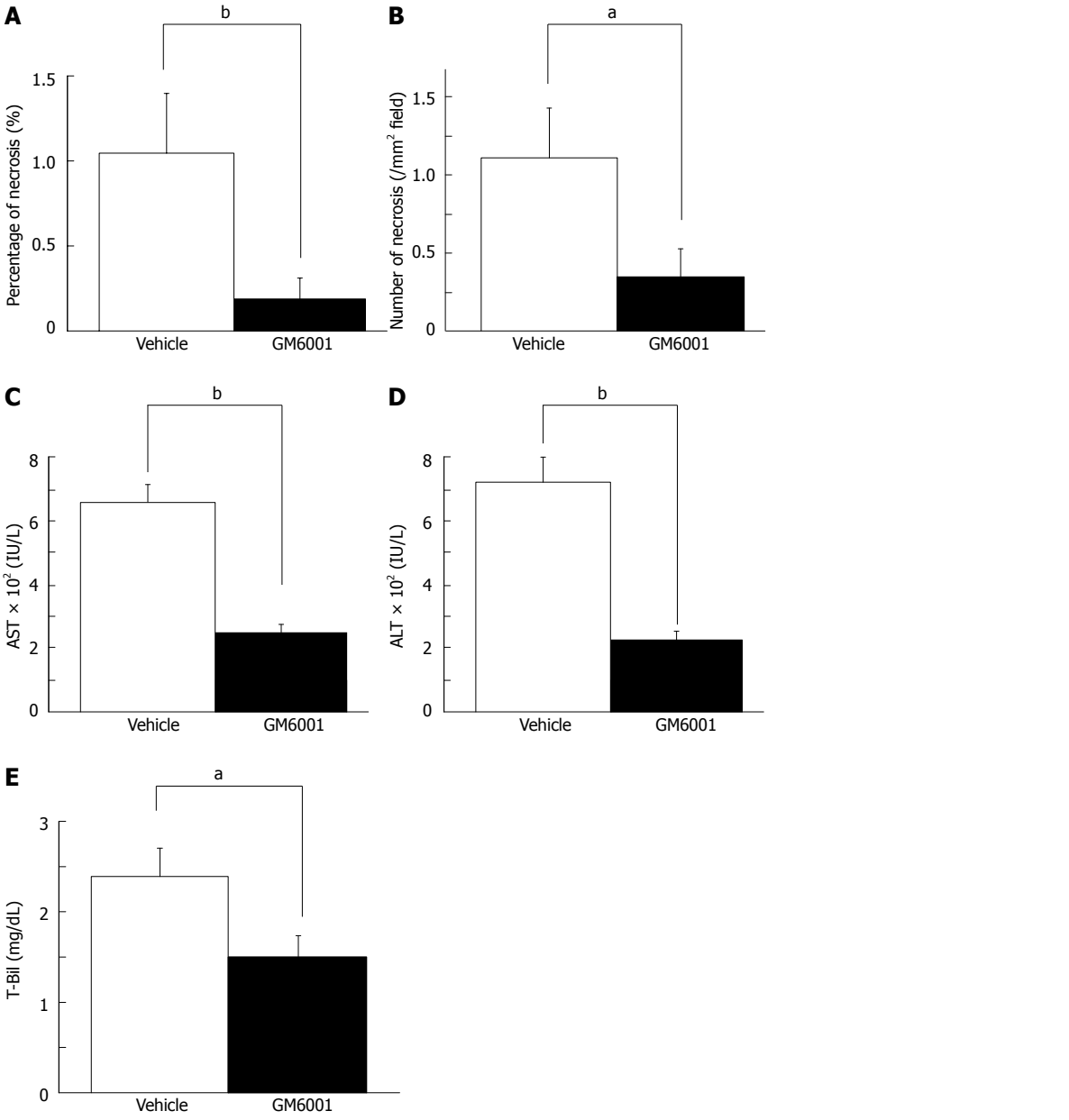
A
b
Percentage of necrosis (%)
1.5
1.0
0.5
0
Vehicle
GM6001
B
a
Number of necrosis (/mm2 field)
1.5
1.0
0.5
0
Vehicle
GM6001
C
b
AST × 10^2 (IU/L)
8
6
4
2
0
Vehicle
GM6001
D
b
ALT × 10^2 (IU/L)
8
6
4
2
0
Vehicle
GM6001
E
a
T-Bil (mg/dL)
3
2
1
0
Vehicle
GM6001

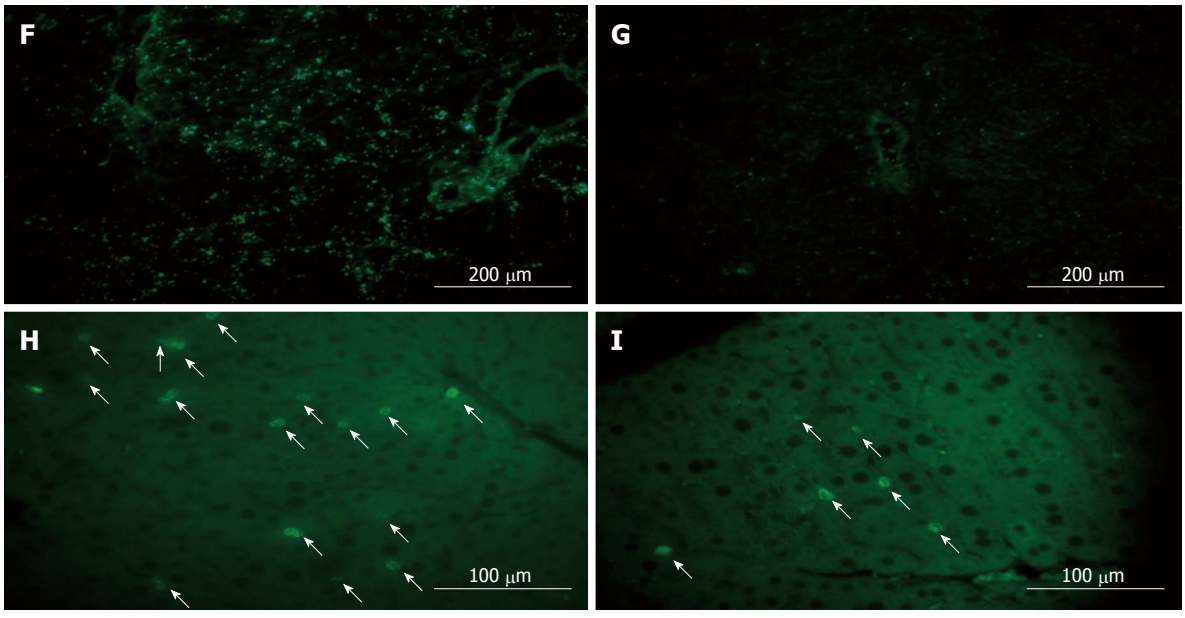
F
200 μm
G
200 μm
H
100 μm
I
100 μm

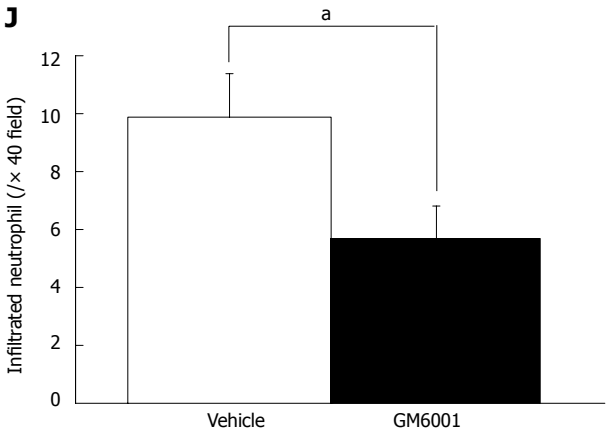

Figure 9 Broad-spectrum matrix metalloproteinase-9 inhibitor GM6001 ameliorate initial injury of the liver 6 h after 80%-partial hepatectomy. We inhibited matrix metalloproteinase-9 by GM6001 in 80%-partial hepatectomy (PH) mice, and determined liver necrosis 6 h after 80%-PH. Liver damage was significantly reduced in the GM6001-treated mice compared with that in the vehicle-treated group (A, B). Serum levels of aspartate aminotransferase (AST) (C), alamine aminotransferase (ALT) (D) and total bilirubin (T-Bil) (E) were significantly lower in the GM6001-treated mice than those in the vehicle-treated mice. Representative images of *in situ* gelatin zymography analysis with DQ gelatin are shown. Gelatinolytic activity was suppressed in the GM6001-treated mice (G) compared with that in the vehicle-treated mice (F). Representative images of myeloperoxidase staining on remnant liver (RL) sections in vehicle-treated mice (H) and GM6001-treated mice (I) are shown. A histogram of the number of accumulated neutrophils in the RL after extended hepatectomy shows that there are significantly fewer neutrophils in the GM6001-treated mice than in the vehicle-treated mice (J) ($^{a}P < 0.05$, $^{b}P < 0.01$ *vs* vehicle-treated mice).

fewer accumulated neutrophils in the mAb group than in the control IgG group (mAb: 4.2 ± 1.2 *vs* control IgG: 9.6 ± 1.9, each per 40 high-power field, $P < 0.05$) (Figure 8E-G).

Similarly, the inhibition study by GM6001 showed a significant suppression in the area of liver necrosis (1.04% ± 0.36% *vs* 0.19% ± 0.13%, $P < 0.01$, Figure 9A) and the number of foci compared with the vehicle group (1.12 ± 0.31/mm^2 *vs* 0.35 ± 0.19/mm^2, $P < 0.05$, Figure 9B). The levels of AST (660 ± 66 IU/L *vs* 243 ± 28 IU/L, $P < 0.01$, Figure 9C), ALT (702 ± 88 IU/L *vs* 212 ± 33 IU/L, $P < 0.01$, Figure 9D) and T-Bil (1.49 ± 0.25 mg/dL *vs* 2.39 ± 0.30 mg/dL, $P < 0.05$, Figure 9E) were significantly lower in the GM6001 group than those in the vehicle group. *In situ* gelatin zymography analysis indicated inhibition of gelatinolytic activity in the GM6001 group (Figure 9F-I). Additionally, the accumulation of neutrophils was significantly suppressed in the GM6001 group compared with the vehicle group (9.9 ± 1.5 per 40 high-power field *vs* 5.7 ± 1.1 per 40 high-power field, $P < 0.05$) (Figure 9J). These results suggested that therapy with exogenous MMP-9 inhibition has the potential to reduce the initial injury of RL after EH.

DISCUSSION

The mechanism of PLF is not fully understood, because of the involvement of various clinical perioperative factors, such as pre-existing liver disease, infection, transfusion, and insufficient volume of the RL. Murine and rat models have been used to determine the mechanisms for many years. Jin *et al*[15] showed necrosis of hepatocytes by oxidative injury after 87%-PH in mice. Catardegirmen *et al*[22] reported that blockage of the receptor for advanced glycation end products (RAGE) improves survival after 85%-PH and preserves liver parenchyma with the absence of necrosis in 85%-PH. Yoshida *et al*[23] reported the efficiency of a caspase inhibitor for survival after 95%-PH in rats by attenuating apoptosis of hepatocytes. Both necrosis and apoptosis pathways appear to be involved in PLF process after EH. We previously performed marginal hepatectomy to evaluate the difference between predictive liver failure and normal recovery at the early phase. Use of hemoclips and a surgical microscope enabled us to complete the surgical procedure within 10 min and to stabilize the outcomes after surgery in our model[12]. In this previous study, a quick procedure appeared to reduce the opportunity for an infection or any complications[12]. In our preliminary study, histological changes from 80%-PH[12] were slightly improved compared with a conventional model by Higgins *et al*[24]. Our marginal PH model could be helpful for evaluation of the direct effects of insufficient volume of the RL after EH, from the viewpoint of the deletions of irrelevant factors.

With regard to the mechanism of liver failure, only a few studies have focused on the initial changes in the RL after EH. Panis *et al*[16] reported the presence of centrilobular necrosis, which varied in the severity in different areas of sections as well as a fatty change and microvascular steatosis 24 h after 85%-PH in the rat. Jin *et al*[15] reported severe sinusoidal narrowing as early as 6 h, and swelling, fatty degeneration and nuclear condensation of hepatocytes by 48 h after 87%-PH in asymptomatic mice[15]. In small-for-size grafts used in transplantation, a vacuolar cytoplasm or considerable mitochondrial swelling in hepatocytes, irregular large gaps between sinusoidal lining cells and collapse of the space of Disse have been observed[25]. Our study clearly showed multiple necroses with intrahepatic-hemorrhage in the RL, and biochemical results also revealed PLF at the early phase after 80%-PH in symptomatic mice. In-

terestingly, these histological changes were similar to the findings of a lipopolysaccharide/galactosamine-induced acute liver failure model[26]. Initial extravasation of red blood cells, sinusoidal congestion, destruction of parenchymal architecture and subsequent total destruction of micro-architecture with hemorrhage were reported 4 to 8 h after a challenge of galactosamine and lipopolysaccharide[26]. We also observed dehiscence of sinusoids 6 h after 80%-PH. The mechanism of sinusoidal cell injury is not fully understood. Many efforts after PH, such as hyperperfusion and shear stress due to portal hypertension, appear to have the potential to physically damage sinusoidal endothelial cells (SECs), and intensive decompression of the portal vein has recently been proposed as an intra-operative strategy for liver transplantation with small-for-size grafts[27]. We observed distention of the portal vein during 80%-PH. An increase in portal flow indicates an increased exposure of bacterial products or toxic agents from the gut for an insufficient RL after EH, and this condition may affect SECs. The development of SEC injury followed by parenchymal cell injury is considered as an important mechanism in monocrotaline-induced veno-occlusive disease or acetaminophen hepatotoxicity[28-30], because SEC injury leads to hepatic microcirculatory dysfunction and hemorrhage[28,29]. SEC gap formation after treatment with galactosamine/endotoxin in mice has been reported to affect neutrophil extravasation and hemorrhage of liver parenchyma, and activated MMP is involved in SEC gap formation[31]. MMPs have been shown to be involved in several liver injury mechanisms including the fulminant liver failure model[32], sinusoidal obstruction syndrome model[33] and hepatic ischemia/reperfusion injury model[20]. Olle *et al*[34] have reported the importance of MMP-9 associated with tumor necrosis factor, hepatocyte growth factor, vascular endothelial growth factor and the apoptosis pathway for liver regeneration. Mohammed *et al*[35] showed that TIMP-1 affects the hepatocyte cell cycle in the liver regeneration process. These findings indicate MMPs' negative and positive potential in liver disease. A RL with considerable damage requires emergent regeneration for survival after EH. The role of MMPs appears to be more complex.

We demonstrated that MMP-9 expression was enhanced in the damaged liver associated with necrosis, and the main source of MMP-9 was CD11b-positive nonnative leukocytes and hepatic stellate cells 6 h after 80%-PH. Our results appear to be consistent with the ischemia/reperfusion injury model and acute liver failure model[26]. Kim *et al*[36] showed initial MMP-9 expression at 3 h in only periportal hepatocytes after 70%-PH in the rat, and positive staining gradually spread for up to 48 h. In our 80%-PH model, there was little expression of MMP-9 in hepatocytes 6 h after surgery, and our results suggested that a severe situation after 80%-PH impairs the regular process for normal regeneration observed after 70%-PH[13,36]. Yan *et al*[26] showed bimodal alteration of MMP-9 mRNA in the acute liver failure model. We observed a change in bimodal activity (the second peak was after 12 h) by zymography after 80%-PH (data not shown). Taken together, these results suggest that there are two different modalities for MMP-9 production. Although we previously reported that MMP-9 plays an important role in the development of parenchymal hemorrhage and necrosis in the small remnant liver after massive hepatectomy and that successful MMP-9 inhibition attenuates the formation of hemorrhage and necrosis and might be a potential therapy to ameliorate liver injury[11], the origin of MMP-9 production was unclear. We speculate that it is necessary to separately consider the roles of MMP-9 produced from leukocytes at the early phase and from hepatocytes at the late phase of EH.

In the current study, we focused on the initial MMP-9 expression and hypothesized that it plays a role in liver injury in the RL after EH. To examine the involvement of MMP-9 in initial liver injury after EH, we evaluated the effect of inhibition of MMP-9 using three different methods *in vivo* including MMP-9-deficient mice, an inhibitory monoclonal antibody and a broad spectrum inhibitor. In all of the MMP-9 inhibitory experiments, suppression of the initial injury was clearly observed with the inhibition of MMP-9. Our results suggested that MMP-9 plays a pivotal role in liver injury, especially in the formation of necrosis, likely sinusoidal injury after 80%-PH. Perioperative factors in each experiment were not different between each experimental group such as the resected volume, the surgical time and intra-operative blood loss. In the experiments with genetic deficient mice, we examined whether TIMP-1 deficiency had any effects on the theoretical enhancement of MMP-9 activity on liver injury simultaneously. We observed the reverse effects in TIMP-1 deficient mice compared with MMP-9-deficient mice with an increased gelatinolytic activity. No exacerbation of liver injury in the TIMP-1-deleted condition suggested insufficiency of TIMP-1 to regulate MMP-9 activity after EH. Mohammed *et al*[35] showed that TIMP-1 was slightly increased 6 to 18 h after 70%-PH in the rat. We did not assess TIMP-1 expression in the current study. However, it is possible that TIMP-1 could be used as a therapeutic target to reduce MMP-9 levels related to liver injury.

In the current study, we did not observe any survival benefits of MMP-9 inhibition in MMP-9(-/-) mice, although the other two methods of inhibition of MMP-9 showed improvement of survival. MMP-9 was shown to be important in liver regeneration in PH by Olle *et al*[34]. Additionally, the possibility of impairment of the host defense by MMP-9 deficiency was reported in a sepsis model by Renckens *et al*[37]. Excessive MMP-9 activity induced by shear stress after PH may have the potential to induce initial liver injury. Application of MMP-9 blockade should be precisely controlled.

In this study, we evaluated the accumulation of neutrophils in the RL after 80%-PH. Areas of necrosis were correlated with the number of accumulated neutrophils. The infiltration of polymorphonuclear neutrophils (PMNs) has been reported in several liver diseases[38-41] and even after EH[42]. We could not identify infiltrated

neutrophils as a central effecter on liver injury after 80%-PH, but a possible explanation may be provided by an association between neutrophils and SEC destruction. In addition, recent studies have shown that MMP-9 derived from neutrophils affects several pathophysiological conditions such as blood brain barrier breakdown after an ischemic stroke and gut barrier dysfunction in an acute pancreatitis model[43,44]. Keck *et al*[45] showed that PMN-derived MMP-9 contributes to the accumulation of PMNs in the inflammation site and it initiates damage to the basement membrane. Although our results are consistent with the previous work described above, the mechanism of liver damage or regeneration is complicate. Periportal infiltration of inflammatory cells will increase the liver damage, but this infiltration is paradoxically necessary to trigger the liver regeneration[46-48]. Though the balance of damage and regeneration is still unclear, we speculated that the MMP-9 produced from neutrophil may be important factor for a successful liver regeneration after EH. Further study is needed to elucidate the involvement of MMP-9 associated with neutrophils in liver injury after EH with an insufficient RL.

In summary, our data showed that the pathway of liver necrosis related to initial sinusoidal endothelial cell injury is responsible for the PLF process after EH with an insufficient RL. The initial injury is associated with MMP-9 derived from neutrophils, and blockade of MMP-9 reduces initial liver injury in an *in vivo* model. Our results suggest that MMP-9 may be a potential target for preventive care or further challenging for EH.

ACKNOWLEDGMENTS

We are grateful to Dennis W Dickson, Monica Castanedes-Casey, Virginia R Phillips, Linda G Rousseau and Melissa E Murray (Department of Neuroscience, Mayo Clinic in Florida, Jacksonville, FL 32224, United States) for their technical support with histopathological assessment.

COMMENTS

Background

Postoperative liver failure (PLF) after extended hepatectomy (EH) can cause an insufficient volume of the remnant liver (RL), resulting in higher morbidity and mortality.

Research frontiers

The mechanism of liver damage or regeneration is complicate. Periportal infiltration of inflammatory cells will increase the liver damage, but this infiltration is paradoxically necessary to trigger the liver regeneration. This PLF is progressive from the early postoperative period, but the mechanism is unknown. Authors hypothesized that matrix metalloproteinase (MMP)-9 plays a role in PLF pathogenesis.

Innovations and breakthroughs

Though the balance of damage and regeneration is still unclear in the RL after EH, the MMP-9 produced from neutrophil may be important factor for a successful liver regeneration after EH.

Applications

Their data showed that the pathway of liver necrosis related to initial sinusoidal endothelial cell injury is responsible for the PLF process after EH. The initial injury is associated with MMP-9 derived from neutrophils, and blockade of MMP-9 reduces initial liver injury.

Terminology

Their results suggest that MMP-9 may be a potential target for preventive care or further challenging for EH.

Peer review

In this manuscript, authors attempt to investigate that the effect of MMP9 in the initial injury after hepatectomy in mice. The work is of potential interest to the readership of the *World Journal of Gastroenterology*.

REFERENCES

1 **Bachellier P**, Rosso E, Pessaux P, Oussoultzoglou E, Nobili C, Panaro F, Jaeck D. Risk factors for liver failure and mortality after hepatectomy associated with portal vein resection. *Ann Surg* 2011; **253**: 173-179 [PMID: 21233614 DOI: 10.1097/SLA.0b013e3181f193ba]

2 **Fan ST**, Mau Lo C, Poon RT, Yeung C, Leung Liu C, Yuen WK, Ming Lam C, Ng KK, Ching Chan S. Continuous improvement of survival outcomes of resection of hepatocellular carcinoma: a 20-year experience. *Ann Surg* 2011; **253**: 745-758 [PMID: 21475015 DOI: 10.1097/SLA.0b013e3182111195]

3 **Mei Y**, Thevananther S. Endothelial nitric oxide synthase is a key mediator of hepatocyte proliferation in response to partial hepatectomy in mice. *Hepatology* 2011; **54**: 1777-1789 [PMID: 21748771 DOI: 10.1002/hep.24560]

4 **Ma ZY**, Qian JM, Rui XH, Wang FR, Wang QW, Cui YY, Peng ZH. Inhibition of matrix metalloproteinase-9 attenuates acute small-for-size liver graft injury in rats. *Am J Transplant* 2010; **10**: 784-795 [PMID: 20121733 DOI: 10.1111/j.1600-6143.2009.02993.x]

5 **Defamie V**, Laurens M, Patrono D, Devel L, Brault A, Saint-Paul MC, Yiotakis A, Barbry P, Gugenheim J, Crenesse D, Dive V, Huet PM, Mari B. Matrix metalloproteinase inhibition protects rat livers from prolonged cold ischemia-warm reperfusion injury. *Hepatology* 2008; **47**: 177-185 [PMID: 18008367 DOI: 10.1002/hep.21929]

6 **Zhang Y**, Dong J, He P, Li W, Zhang Q, Li N, Sun T. Genistein inhibit cytokines or growth factor-induced proliferation and transformation phenotype in fibroblast-like synoviocytes of rheumatoid arthritis. *Inflammation* 2012; **35**: 377-387 [PMID: 21792602 DOI: 10.1007/s10753-011-9365-x]

7 **Heo SH**, Cho CH, Kim HO, Jo YH, Yoon KS, Lee JH, Park JC, Park KC, Ahn TB, Chung KC, Yoon SS, Chang DI. Plaque rupture is a determinant of vascular events in carotid artery atherosclerotic disease: involvement of matrix metalloproteinases 2 and 9. *J Clin Neurol* 2011; **7**: 69-76 [PMID: 21779294 DOI: 10.3988/jcn.2011.7.2.69]

8 **Zhang B**, Halder SK, Kashikar ND, Cho YJ, Datta A, Gorden DL, Datta PK. Antimetastatic role of Smad4 signaling in colorectal cancer. *Gastroenterology* 2010; **138**: 969-980.e1-3 [PMID: 19909744 DOI: 10.1053/j.gastro.2009.11.004]

9 **Ke AW**, Shi GM, Zhou J, Wu FZ, Ding ZB, Hu MY, Xu Y, Song ZJ, Wang ZJ, Wu JC, Bai DS, Li JC, Liu KD, Fan J. Role of overexpression of CD151 and/or c-Met in predicting prognosis of hepatocellular carcinoma. *Hepatology* 2009; **49**: 491-503 [PMID: 19065669 DOI: 10.1002/hep.22639]

10 **Padrissa-Altés S**, Zaouali MA, Franco-Gou R, Bartrons R, Boillot O, Rimola A, Arroyo V, Rodés J, Peralta C, Roselló-Catafau J. Matrix metalloproteinase 2 in reduced-size liver transplantation: beyond the matrix. *Am J Transplant* 2010; **10**: 1167-1177 [PMID: 20353474 DOI: 10.1111/j.1600-6143.2010.03092.x]

11 **Ohashi N**, Hori T, Chen F, Jermanus S, Eckman CB, Nakao A, Uemoto S, Nguyen JH. Matrix metalloproteinase-9 contributes to parenchymal hemorrhage and necrosis in the remnant liver after extended hepatectomy in mice. *World J Gastroenterol* 2012; **18**: 2320-2333 [PMID: 22654423 DOI: 10.3748/wjg.v18.i19.2320]

12 **Hori T**, Ohashi N, Chen F, Baine AM, Gardner LB, Hata T, Uemoto S, Nguyen JH. Simple and reproducible hepatectomy in the mouse using the clip technique. *World J Gastroenterol* 2012; **18**: 2767-2774 [PMID: 22719184 DOI: 10.3748/wjg.v18.i22.2767]

13 **Mitchell C**, Willenbring H. A reproducible and well-tolerated method for 2/3 partial hepatectomy in mice. *Nat Protoc* 2008; **3**: 1167-1170 [PMID: 18600221 DOI: 10.1038/nprot.2008.80]

14 **Rudich N**, Zamir G, Pappo O, Shlomai Z, Faroja M, Weiss ID, Wald H, Galun E, Peled A, Wald O. Focal liver necrosis appears early after partial hepatectomy and is dependent on T cells and antigen delivery from the gut. *Liver Int* 2009; **29**: 1273-1284 [PMID: 19538448 DOI: 10.1111/j.1478-3231.2009.02048.x]

15 **Jin X**, Zhang Z, Beer-Stolz D, Zimmers TA, Koniaris LG. Interleukin-6 inhibits oxidative injury and necrosis after extreme liver resection. *Hepatology* 2007; **46**: 802-812 [PMID: 17668886 DOI: 10.1002/hep.21728]

16 **Panis Y**, McMullan DM, Emond JC. Progressive necrosis after hepatectomy and the pathophysiology of liver failure after massive resection. *Surgery* 1997; **121**: 142-149 [PMID: 9037225]

17 **Matkowskyj KA**, Marrero JA, Carroll RE, Danilkovich AV, Green RM, Benya RV. Azoxymethane-induced fulminant hepatic failure in C57BL/6J mice: characterization of a new animal model. *Am J Physiol* 1999; **277**: G455-G462 [PMID: 10444460]

18 **Bélanger M**, Côté J, Butterworth RF. Neurobiological characterization of an azoxymethane mouse model of acute liver failure. *Neurochem Int* 2006; **48**: 434-440 [PMID: 16563565 DOI: 10.1016/j.neuint.2005.11.022]

19 **Zhong Z**, Connor HD, Froh M, Bunzendahl H, Lind H, Lehnert M, Mason RP, Thurman RG, Lemasters JJ. Free radical-dependent dysfunction of small-for-size rat liver grafts: prevention by plant polyphenols. *Gastroenterology* 2005; **129**: 652-664 [PMID: 16083719 DOI: 10.1053/j.gastro.2005.05.060]

20 **Hamada T**, Fondevila C, Busuttil RW, Coito AJ. Metalloproteinase-9 deficiency protects against hepatic ischemia/reperfusion injury. *Hepatology* 2008; **47**: 186-198 [PMID: 17880014 DOI: 10.1002/hep.21922]

21 **Brown KE**, Brunt EM, Heinecke JW. Immunohistochemical detection of myeloperoxidase and its oxidation products in Kupffer cells of human liver. *Am J Pathol* 2001; **159**: 2081-2088 [PMID: 11733358]

22 **Cataldegirmen G**, Zeng S, Feirt N, Ippagunta N, Dun H, Qu W, Lu Y, Rong LL, Hofmann MA, Kislinger T, Pachydaki SI, Jenkins DG, Weinberg A, Lefkowitch J, Rogiers X, Yan SF, Schmidt AM, Emond JC. RAGE limits regeneration after massive liver injury by coordinated suppression of TNF-alpha and NF-kappaB. *J Exp Med* 2005; **201**: 473-484 [PMID: 15699076 DOI: 10.1084/jem.20040934]

23 **Yoshida N**, Iwata H, Yamada T, Sekino T, Matsuo H, Shirahashi K, Miyahara T, Kiyama S, Takemura H. Improvement of the survival rate after rat massive hepatectomy due to the reduction of apoptosis by caspase inhibitor. *J Gastroenterol Hepatol* 2007; **22**: 2015-2021 [PMID: 17559362 DOI: 10.1111/j.1440-1746.2007.04960.x]

24 **Higgins G**, Anderson R. Experimental pathology of the liver. Restoration of the liver of the white rat following partial surgical removal. *Arch Pathol* 1931; **12**: 186-202

25 **Man K**, Lo CM, Ng IO, Wong YC, Qin LF, Fan ST, Wong J. Liver transplantation in rats using small-for-size grafts: a study of hemodynamic and morphological changes. *Arch Surg* 2001; **136**: 280-285 [PMID: 11231846 DOI: 10.1001/archsurg.136.3.280]

26 **Yan C**, Zhou L, Han YP. Contribution of hepatic stellate cells and matrix metalloproteinase 9 in acute liver failure. *Liver Int* 2008; **28**: 959-971 [PMID: 18507761 DOI: 10.1111/j.1478-3231.2008.01775.x]

27 **Yamada T**, Tanaka K, Uryuhara K, Ito K, Takada Y, Uemoto S. Selective hemi-portocaval shunt based on portal vein pressure for small-for-size graft in adult living donor liver transplantation. *Am J Transplant* 2008; **8**: 847-853 [PMID: 18261170 DOI: 10.1111/j.1600-6143.2007.02144.x]

28 **DeLeve LD**, McCuskey RS, Wang X, Hu L, McCuskey MK, Epstein RB, Kanel GC. Characterization of a reproducible rat model of hepatic veno-occlusive disease. *Hepatology* 1999; **29**: 1779-1791 [PMID: 10347121]

29 **Ito Y**, Bethea NW, Abril ER, McCuskey RS. Early hepatic microvascular injury in response to acetaminophen toxicity. *Microcirculation* 2003; **10**: 391-400 [PMID: 14557822]

30 **Ito Y**, Bethea NW, Baker GL, McCuskey MK, Urbaschek R, McCuskey RS. Hepatic microcirculatory dysfunction during cholestatic liver injury in rats. *Microcirculation* 2003; **10**: 421-432 [PMID: 14557825 DOI: 10.1038/sj.mn.7800208]

31 **Ito Y**, Abril ER, Bethea NW, McCuskey MK, Cover C, Jaeschke H, McCuskey RS. Mechanisms and pathophysiological implications of sinusoidal endothelial cell gap formation following treatment with galactosamine/endotoxin in mice. *Am J Physiol Gastrointest Liver Physiol* 2006; **291**: G211-G218 [PMID: 16574994 DOI: 10.1152/ajpgi.00312.2005]

32 **Wielockx B**, Lannoy K, Shapiro SD, Itoh T, Itohara S, Vandekerckhove J, Libert C. Inhibition of matrix metalloproteinases blocks lethal hepatitis and apoptosis induced by tumor necrosis factor and allows safe antitumor therapy. *Nat Med* 2001; **7**: 1202-1208 [PMID: 11689884 DOI: 10.1038/nm1101-1202]

33 **Deleve LD**, Wang X, Tsai J, Kanel G, Strasberg S, Tokes ZA. Sinusoidal obstruction syndrome (veno-occlusive disease) in the rat is prevented by matrix metalloproteinase inhibition. *Gastroenterology* 2003; **125**: 882-890 [PMID: 12949732 DOI: 10.1016/S0016-5085(03)01056-4]

34 **Olle EW**, Ren X, McClintock SD, Warner RL, Deogracias MP, Johnson KJ, Colletti LM. Matrix metalloproteinase-9 is an important factor in hepatic regeneration after partial hepatectomy in mice. *Hepatology* 2006; **44**: 540-549 [PMID: 16941692 DOI: 10.1002/hep.21314]

35 **Mohammed FF**, Pennington CJ, Kassiri Z, Rubin JS, Soloway PD, Ruther U, Edwards DR, Khokha R. Metalloproteinase inhibitor TIMP-1 affects hepatocyte cell cycle via HGF activation in murine liver regeneration. *Hepatology* 2005; **41**: 857-867 [PMID: 15726641 DOI: 10.1002/hep.20618]

36 **Kim TH**, Mars WM, Stolz DB, Michalopoulos GK. Expression and activation of pro-MMP-2 and pro-MMP-9 during rat liver regeneration. *Hepatology* 2000; **31**: 75-82 [PMID: 10613731]

37 **Renckens R**, Roelofs JJ, Florquin S, de Vos AF, Lijnen HR, van't Veer C, van der Poll T. Matrix metalloproteinase-9 deficiency impairs host defense against abdominal sepsis. *J Immunol* 2006; **176**: 3735-3741 [PMID: 16517742]

38 **Jaeschke H**, Farhood A, Smith CW. Neutrophils contribute to ischemia/reperfusion injury in rat liver in vivo. *FASEB J* 1990; **4**: 3355-3359 [PMID: 2253850]

39 **Doi F**, Goya T, Torisu M. Potential role of hepatic macrophages in neutrophil-mediated liver injury in rats with sepsis. *Hepatology* 1993; **17**: 1086-1094 [PMID: 8099895]

40 **Ramaiah SK**, Jaeschke H. Role of neutrophils in the pathogenesis of acute inflammatory liver injury. *Toxicol Pathol* 2007; **35**: 757-766 [PMID: 17943649 DOI: 10.1080/01926230701584163]

41 **Jaeschke H**, Hasegawa T. Role of neutrophils in acute inflammatory liver injury. *Liver Int* 2006; **26**: 912-919 [PMID: 16953830 DOI: 10.1111/j.1478-3231.2006.01327.x]

42 **Ohtsuka M**, Miyazaki M, Kondo Y, Nakajima N. Neutrophil-mediated sinusoidal endothelial cell injury after extensive hepatectomy in cholestatic rats. *Hepatology* 1997; **25**: 636-641 [PMID: 9049211]

43 **Mikami Y**, Dobschütz EV, Sommer O, Wellner U, Unno M, Hopt U, Keck T. Matrix metalloproteinase-9 derived from

polymorphonuclear neutrophils increases gut barrier dysfunction and bacterial translocation in rat severe acute pancreatitis. *Surgery* 2009; **145**: 147-156 [PMID: 19167969 DOI: 10.1016/j.surg.2008.08.036]

44 **Rosell A**, Cuadrado E, Ortega-Aznar A, Hernández-Guillamon M, Lo EH, Montaner J. MMP-9-positive neutrophil infiltration is associated to blood-brain barrier breakdown and basal lamina type IV collagen degradation during hemorrhagic transformation after human ischemic stroke. *Stroke* 2008; **39**: 1121-1126 [PMID: 18323498 DOI: 10.1161/STROKEAHA.107.500868]

45 **Keck T**, Balcom JH, Fernández-del Castillo C, Antoniu BA, Warshaw AL. Matrix metalloproteinase-9 promotes neutrophil migration and alveolar capillary leakage in pancreatitis-associated lung injury in the rat. *Gastroenterology* 2002; **122**: 188-201 [PMID: 11781293]

46 **Jaeschke H**. Mechanisms of Liver Injury. II. Mechanisms of neutrophil-induced liver cell injury during hepatic ischemia-reperfusion and other acute inflammatory conditions. *Am J Physiol Gastrointest Liver Physiol* 2006; **290**: G1083-G1088 [PMID: 16687579 DOI: 10.1152/ajpgi.00568.2005]

47 **Plümpe J**, Streetz K, Manns MP, Trautwein C. Tumour necrosis factor alpha--mediator of apoptosis and cell proliferation of hepatocytes. *Ital J Gastroenterol Hepatol* 1999; **31**: 235-243 [PMID: 10379487]

48 **Jaeschke H**, McGill MR, Williams CD, Ramachandran A. Current issues with acetaminophen hepatotoxicity--a clinically relevant model to test the efficacy of natural products. *Life Sci* 2011; **88**: 737-745 [PMID: 21296090 DOI: 10.1016/j.lfs.2011.01.025]

P- Reviewer Lin JY **S- Editor** Gou SX **L- Editor** A
E- Editor Zhang DN